Struct Multidisc Optim (2017) 55:1517–1534
DOI 10.1007/s00158-016-1585-0

INDUSTRIAL APPLICATION

Drop test simulation and surrogate-based optimization of a dishwasher mechanical structure and its packaging module

O. Mülkoğlu [1,2] · M. A. Güler [1] · E. Acar [1] · H. Demirbağ [1,3]

Received: 18 February 2016 / Revised: 8 August 2016 / Accepted: 5 September 2016 / Published online: 12 October 2016

Abstract A drop test simulation of the mechanical structure of a redesigned dishwasher is performed by using a detailed finite element (FE) model. The nonlinear explicit FE code LS-DYNA® is used for the drop impact simulations. The FE model is validated through real tests of two drop scenarios (vertical and inclined to the side). An optimization study is performed in order to determine the optimum design variables for better crash performance. The effects of geometric parameters and material properties on the weights of certain components (ie, dogleg plate and bottom foam) are investigated. A surrogate-based optimization approach is used to find optimum values for the dogleg plate thickness, bottom foam density and increment of the bottom foam height to minimize the weights of both components. Two different surrogate models are used to predict optimization problem constraints that have a crucial role in the crash performance of the dishwasher mechanical structure and packaging module: the polynomial response surface and radial basis functions. The results showed that the dogleg plate mass can be slightly reduced and the bottom foam mass can be significantly reduced in order to obtain the optimum dishwasher configuration and better crashworthiness. The weights of the dogleg plate and bottom foam could be lowered by as much as 5.95 and 24.8 %, respectively. Finally, multi-objective optimization is performed by minimizing a composite objective function that provides a compromise between the weights of both components. The results showed that weight reductions of 2.3 and 21.5 % could be obtained for the dogleg plate and bottom foam, respectively.

Keywords Dishwasher · Packaging module · Drop test simulation · Finite element analysis · Surrogate models · Multi-objective optimization

✉ E. Acar
acar@etu.edu.tr

[1] Department of Mechanical Engineering, TOBB University of Economics and Technology, Söğütözü Cad. No:43, Söğütözü, Ankara 06560, Turkey

[2] Department of Mechanical Engineering, Yıldırım Beyazıt University, Ulus, Ankara 06050, Turkey

[3] ARCELIK A.S., Altınordu Cad. No:3 Organize Sanayi Bölgesi, Sincan, Ankara 06935, Turkey

1 Introduction

For customers buying dishwashers, the appearance of the front door and its functional requirements are crucial elements. The durability of the door in every single open state and the weight of the decorative wooden door are some important features for ensuring customer satisfaction. To meet such quality demands, engineers at ARÇELİK AŞ, a leading consumer goods company in Turkey, have redesigned the mechanical structure of a dishwasher. The new structure consists of an integrated stainless steel inner tube with a plastic bottom housing. This new mechanical structure and the packaging module need to be analyzed to determine the critical points in terms of structural integrity.

In the appliance manufacturing industry, the mechanical structure of a prototype is commonly assessed through physical tests such as the static loading, vibration, and drop tests. The freefall/drop test is one such test and is widely used for electronic products. Based on the test results, engineers modify the mechanical structure or packaging module while relying on their experience. This type of design methodology needs many tests to be conducted and is very expensive and time-consuming. Moreover, the quality of the end product is

uncertain (Wang et al. 2005). In order to overcome these problems, finite element (FE) simulations need to be performed in the design stage. The drop of a dishwasher can be analyzed by using simulations to understand the physics of the impact. In addition, FE simulations allow for direct modifications to the design structure.

Explicit nonlinear simulation techniques are ideal for this type of impact situation because the impact occurs within a very short time, so small time steps are needed in order to calculate the contact forces (Wu et al. 1998). However, an explicit simulation with small time steps can be time-intensive. In order to overcome this problem, setting up the simulation properly is crucial; this is a challenging requirement.

There are no freefall or impact test standards for home appliances. Because the usage and transportation of white goods vary depending on the customer and carrier, manufacturers have developed their own standards or instructions based on their experience on how these appliances are transported to customers. Therefore, various drop scenarios have to be carried out. Babu and Biswas (Babu and Biswas 2008) performed drop-and-impact simulations on a waste transfer flask with different drop scenarios, such as dropping on the edges, corners, and base. Other groups have focused on impact simulations for consumer goods such as cookers (Dan 2006), refrigerators (Blanco et al. 2015), and televisions (Low et al. 2004); these simulations also included the packaging module and followed different instructions for the drop tests.

Excluding military standards (MIL-STD-810F 2000; MIL-STD-883F 2004) JEDEC were the first to adopt a standardized methodology (JEDEC Standard JESD22-B11 2003) for board-level drop tests, which are used for handheld electronic devices. Multiple groups have used this standard for drop simulations of test boards (Yeh and Huang 2014), microelectronic devices (Tee et al. 2004, 2005; Wong et al. 2002), and mobile phones (Mattila et al. 2014). Other studies have focused on product-level drop tests and simulations for personal electronic devices such as mobile phones (Wu et al. 1998; Wang et al. 2004; Liu and Li 2011; Hwan et al. 2011) to analyze stress and deformation distributions and generate a mathematical or FE model of the impact.

In addition to such research on electronic products, studies have focused on drop simulations of an airplane (Jackson and Fasanella 2008) or section of an airplane (Jackson and Fasanella 2001) to validate the model through test analysis correlation. Other studies on drop impact analysis have considered different components such as fuel assemblies (Petkevich et al. 2014; Kim et al. 2014) to analyze different drop scenarios and check how the impact force influences the component.

All of these above studies focused on drop impact analysis with different drop situations and validation through real tests. In addition to simulation and validation, the present study aims to determine the optimum design variables for better crash performance by following a surrogate-based optimization approach.

Displacements to the sidewalls and frame of the dishwasher during impact are important variables that should be considered in the design of the mechanical structure. Deformation of the sidewalls is the main reason for the return of many products. Therefore, the maximum displacements to both parts should not exceed the results of the baseline model in the optimization process. Most of the impact energy is absorbed by the packaging module, which should be controlled after the modifications. The effective strain value is inversely proportional to the absorbed energy. Therefore, it should also be checked in order to control the response of the foam during impact.

The main objective of this study is to minimize the weights of certain components by investigating the effects of geometric parameters such as the thickness, and material properties such as the density. Two different drop setups are considered: the vertical drop test and inclined drop test to the side. After the FE analysis (FEA) model was successfully validated based on the experimental results, the critical regions of the mechanical structure and the packaging module are determined for each scenario. Finally, the improved design variables are determined for the most critical setup.

The design of complex engineering systems relies heavily on high-fidelity computer simulations (eg, FE analysis) to predict the system performance. Even though the processing power, memory, and storage capacities of computers have drastically increased over the years, analysis models with acceptable accuracy still have significant computational costs (Venkataraman and Haftka 2004). In this study, FEA of a drop test takes around 20 h of CPU time with an Intel® Xeon® CPU E5-2687 W 0 3.10 GHz processors (two processors) and 32.0 GB RAM. Surrogate-based optimization methods are the most popular approach to addressing problems with a high computational cost (Queipo et al. 2005; Forrester et al. 2008). Commonly used surrogate models include polynomial response surface approximation (Myers and Montgomery 2002), radial basis functions (Buhmann 2003), Kriging (Sacks et al. 1989), neural networks (Smith 1993), and support vector regression (Gunn 1997). Response surface approximation and radial basis functions are used in this study. In the literature, response surface approximation has usually been used to model slightly nonlinear responses, and radial basis functions have usually been used to model fast-changing responses (Jin et al. 2001; Wang et al. 2006). After the surrogate models are constructed, they can be used in a gradient-based optimization algorithm (with multiple starting point) or a global optimization algorithm (usually population based) to solve single-objective or multi-objective optimization problems (Acar et al. 2011; Yildiz and Solanki 2012). In addition to these studies, there are some design optimization examples using reliability-based design optimization for household

appliances such as smart watch (Huang et al. 2015) and smart pad (Huang et al. 2016).

This paper is organized as follows. Section 2 describes the drop test setup and optimization problem. Section 3 presents details on the FE simulations of the dishwasher. Section 4 discusses the surrogate model construction. Section 5 compares the drop test simulations and experimental results and presents the results for the optimization problem. Finally, Section 6 gives the concluding remarks.

2 Problem description

Figure 1 presents examples of accidental drops related to transportation that were considered in this study. The drop height was set to 300 mm for both scenarios. The drop test inclined to the side had an inclination angle of 10° relative to the bottom plate.

The dishwasher structure considered in this study consists of a mechanical structure and packaging module. The bottom foam of the packaging module and dogleg plates in the mechanical structure, which are shown in Fig. 2 (the right part of the model is removed for visualization purposes), are expected to be critical components in the event of an impact. The exploded view of the dishwasher assembly is shown in Fig. 3.

The dogleg plate is one of the critical parts that effect the side wall dent in the event of a drop of a dishwasher. The side wall dent causes most of the returns of the dishwashers produced by ARÇELİK A.Ş., and it is the most critical component to align the door of the dishwasher where the design of the whole assembly starts (F. Ercin, personal communication, May 15, 2015). The foam absorbs 40 % of the total energy in the event of a drop. Therefore, the thickness of the dogleg plate t, the density of the foam ρ, and the increment in the bottom foam height h (see Fig. 4) are selected as design variables. These design variables are optimized to determine the minimum weights of the dogleg plate (W_d) and bottom foam (W_b). The following constraints are used in optimization: (1) the maximum displacement to the side at the dogleg plate u_y,

Fig. 1 Experimental setup: (**a**) Vertical drop test and (**b**) 10° Inclined drop test to the side

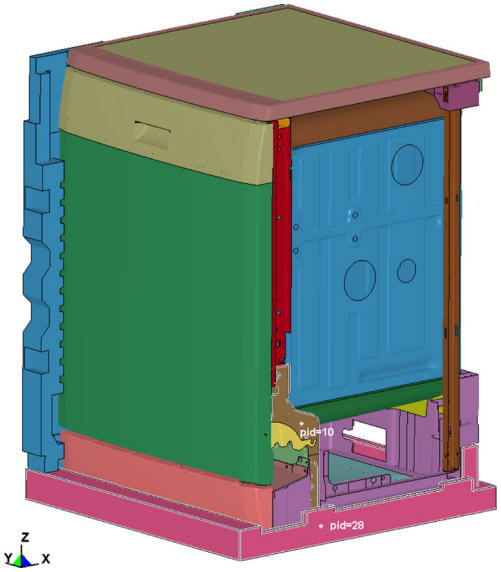

Fig. 2 Dishwasher mechanical structure and its packaging module: dogleg plate ($pid = 10$) and bottom foam ($pid = 28$).

(2) the maximum displacement to the side at the sidewalls v_y, (3) absorbed energy at the bottom foam E_A, and (4) effective strain at the bottom foam E_S. Thus, the optimization problem for minimizing the weight of the dogleg plate or bottom foam can be stated as

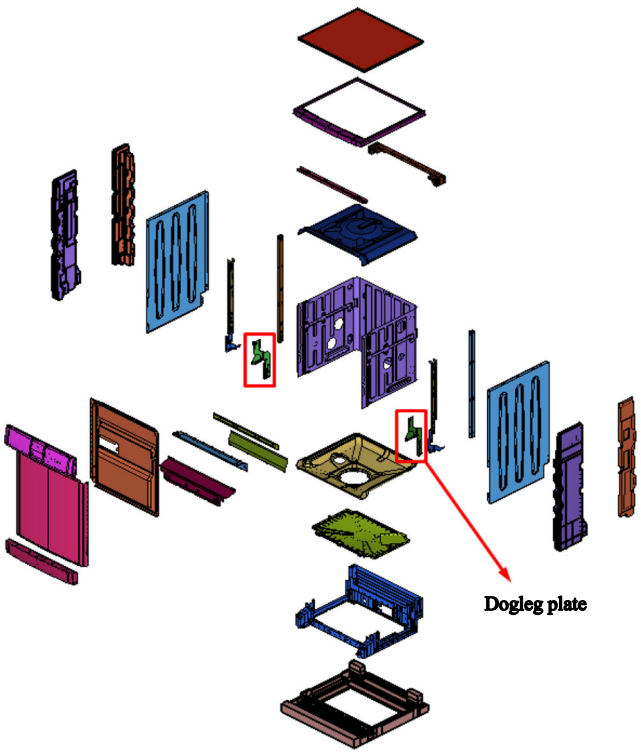

Fig. 3 Exploded view of the dishwasher mechanical structure and its packaging module

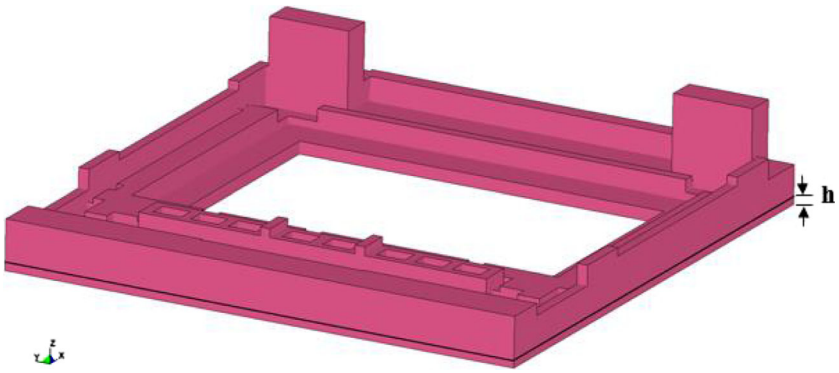

Fig. 4 Increment in the bottom foam height

Find $x = \{t, p, h\}$

Min $W_d(x)(or\ W_b(x))$

Such that

$$u_y(x) \le u_{y-base} \quad (1)$$

$v_y(x) \le v_{y-base}$
$E\_A(x) \ge E\_A_{base}$
$E\_S(x) \le E\_S_{base}$
$1.5 \text{ mm} \le t \le 2.5 \text{ mm}$
$10 \text{ kg/m}^3 \le \rho \le 40 \text{ kg/m}^3$
$0 \le h \le 5 \text{ mm}$

Optimization problems can be solved by using the built-in "fmincon" function of MATLAB (2009 MATLAB user s guide and reference guide The MathWorks Inc 2009), which finds a constrained minimum of a scalar function having several variables by using sequential quadratic programming. To increase the chance of finding the global optimum, optimization runs were started from 100 different randomly generated points.

3 Finite element simulations

There are two numerical solution algorithms for FE simulations: implicit and explicit methods. In drop impact problems, highly nonlinear behavior such as contact and material nonlinearities mean that small time steps are needed. The implicit method is much more time-consuming than the explicit method because of the matrix integration and inversion when small time steps are used (Wu et al. 1998). Therefore, the explicit method is the ideal algorithm for achieving convergence in simulations of drop impact problems. The FE drop simulations in this study are performed by using the nonlinear FE code LS-DYNA.

For efficient FE modeling, geometry cleanup and simplifications are needed for complex structures. Dishwasher structures consist of many different parts that have to be simplified, particularly the geometry of the bottom housing (see Fig. 5). Many small sections should be removed or simplified, such as sharp tips of ribs, fillets on the edges with a small radius, and supporters. Furthermore, parts with negligible effects on the structural behavior such as catchers and small holes should also be simplified.

During the construction of an FE model, some key points affect the accuracy of the simulations. Choosing a proper mesh size that is fine enough to obtain a response at small regions while avoiding small elements is the first step of efficient FE modeling. Because the explicit method is controlled by the smallest element size, a minimum mesh size of 2 mm is used at expected high-stress regions in order to reduce the CPU time for simulations. The FE mesh is generated by using HYPERMESH (HYPERMESH 2009). The overall dishwasher FE model consists of 435,169 shell elements, 963,640 solid elements, and 699 1D rigid and mass elements for a total of 1,399,508 elements. Figure 6 shows the FE model of the dishwasher assembly. Because a fully integrated shell element formulation decreases the analysis time compared to other formulations, it is used for analysis with high computational costs (Livermore Software Technology 2007). Packaging module components are modeled by using hexagonal solid elements. Fully integrated solid elements (S/R solid elements) are selected to prevent excessive distortions that lead to negative Jacobian errors (Bielenberg and Reid 2004).

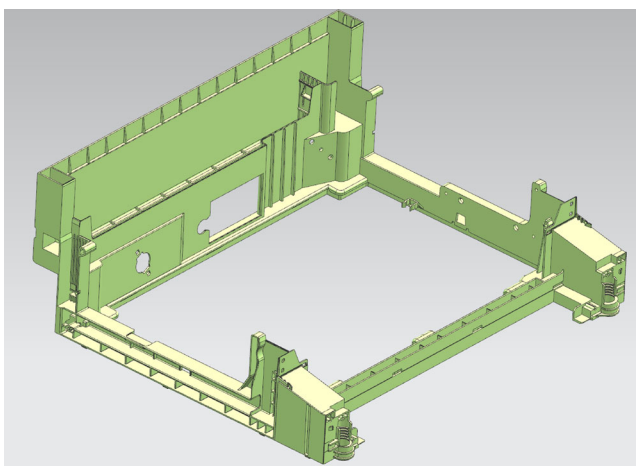

Fig. 5 Geometry of plastic bottom housing

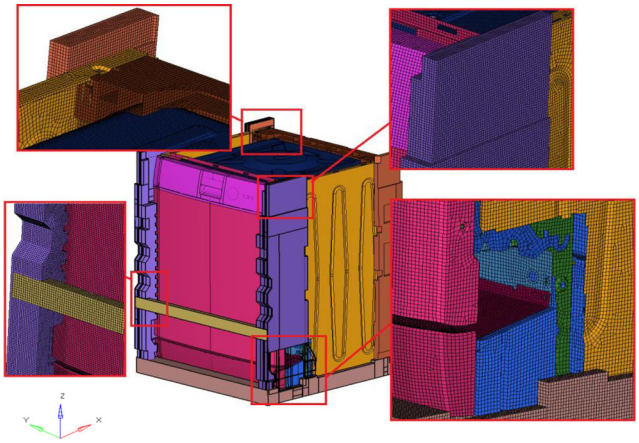

Fig. 6 Finite element model of dishwasher assembly

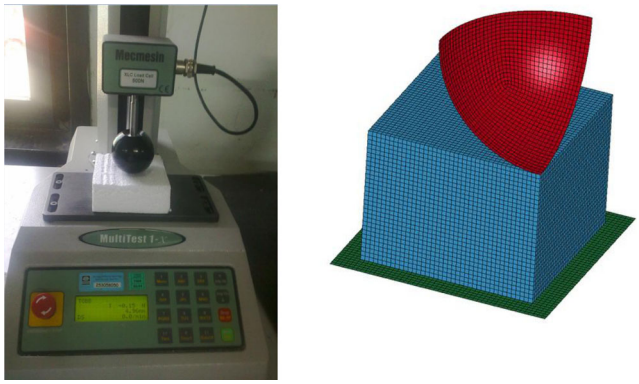

Fig. 7 Material model validation for crushable foam

Choosing a suitable material model and using the correct material properties are another challenge for FE modeling. The elastoplastic material model "Material type 24" is used for the steel parts of the dishwasher. For plastic components such as bottom housing, the elastic–plastic material model "Material type 124," which considers different tensile and compressive stresses versus strain values, is used. In this study, the packaging material and foam has a crucial role in energy absorption. Therefore, it has had to be modeled carefully. As presented in (Mulkoglu et al. 2015), the crushable foam material model "Material type 63" in the LS-DYNA material library was successfully used to model the packaging module. In this study, the material model with the parameters listed in Table 1 is validated (see Fig. 7). Specimens of expanded polystyrene (EPS) crushable foam were compressed into a rigid ball. An FEA simulation of the indentation test for foam was performed, as shown in Fig. 8 (the rigid ball is removed for visualization purposes). In order to minimize the simulation time, a quarter model of the rigid ball and foam block was analyzed. Finally, load–displacement curves were obtained, as shown in Fig. 9. These results proved that the crushable foam material model "Material type 63" with the parameters listed in Table 1 could be used to successfully model the packaging material for the dishwasher.

To define the contact, a single-surface contact algorithm is utilized to consider the self-contact of each part. Contact between the rigid wall and dishwasher is defined with a surface-to-surface contact card provided by LS-DYNA. For each contact definition, the static and dynamic friction coefficients are taken as 0.3 and 0.2, respectively (Acar et al. 2011). For the components on the packaging module, the interface between the support foam and bottom foam is assumed to be fully connected and defined by the "Tied Nodes to Surface" contact algorithm.

4 Constructing surrogate models

The extremely high computational costs of crash simulations are the main challenge for simulation-based optimization. One way to overcome this challenge is to construct surrogate models (or meta-models). The basic concept of surrogate models is constructing a model that can mimic the behavior of the simulation as closely as possible while being computationally efficient. The first step to constructing a surrogate model is to select a design of experiment (DoE) type, which is the sampling plan in design variable space. In this study, a Latin hypercube sampling (LHS) (Park 1994) DoE is used. In the LHS method, the range of values for each variable is divided into l segments. The whole design space consisting of k variables is partitioned into l^k cells, each having equal probability. This study uses three design variables and thirty segments, so 30 cells are chosen as design points, which can be also named training points from the 30^3 cells. After the DoE type is selected, numerical simulations are performed at the training points with LS-DYNA. By computing the responses at the training points, a corresponding pool of response values is generated. Then, the training points and corresponding response values are used to fit a surrogate model that could estimate the response at any arbitrary point within

Table 1 Parameters of input card for crushable foam material model

Parameter	Description	Value	Units
RO	Density	$2.2 \times (10)^{-11}$	Tonne/mm^3
E	Young's Modulus	78	MPa
PR	Poisson's ratio	0	
TSC	Tensile stress cut-off	0.1	MPa
DAMP	Rate sensitivity via damping coefficient	0.5	

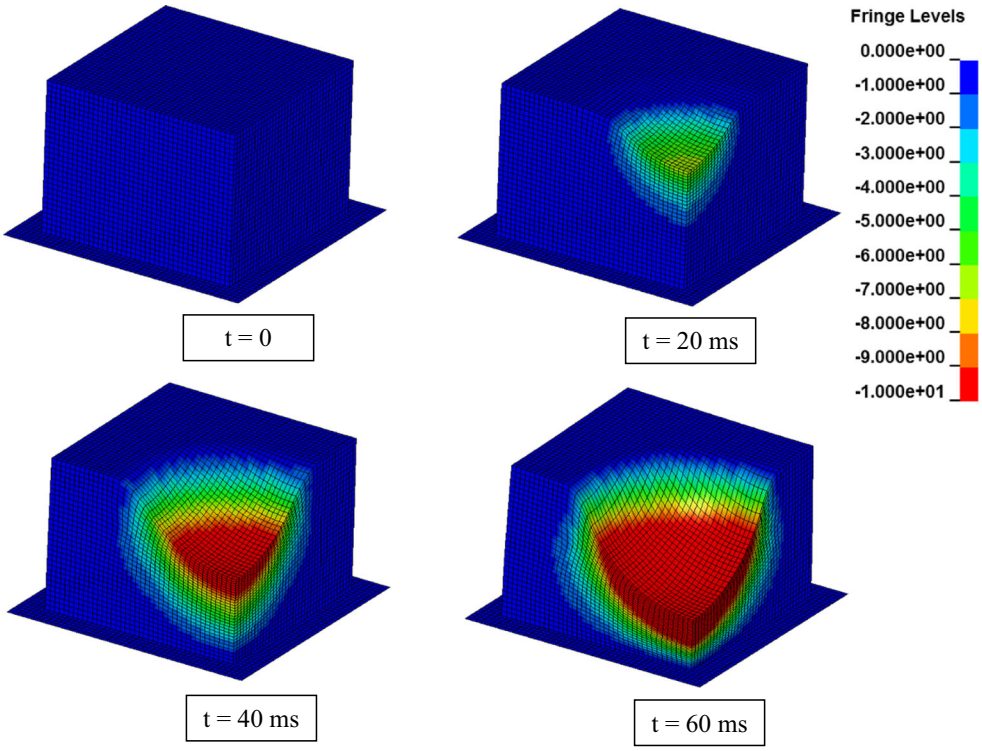

Fig. 8 FEA results of indentation test (z-displacement contour in mm)

the bounds of the input variables. Polynomial response surface (PRS) approximation and radial basis functions (RBFs) are used as different types of surrogate models.

The most commonly used PRS approximation is a second-order model in the form of a second-degree algebraic polynomial function (Myers and Montgomery 2002):

$$\hat{y}(x) = a_0 + \sum_{i=1}^{N} a_i x_i + \sum_{i=1}^{N} a_{ii} x_i^2 + \sum_{i=1}^{N-1} \sum_{j=i+1}^{N} a_{ij} x_i x_j, \qquad (2)$$

where $\hat{y}$ is the response surface approximation of the actual response function y, N is the number of variables, x is the input vector, and a_0, a_i, a_{ii}, a_{ij} are the unknown coefficients to be determined by means of the least-squares method.

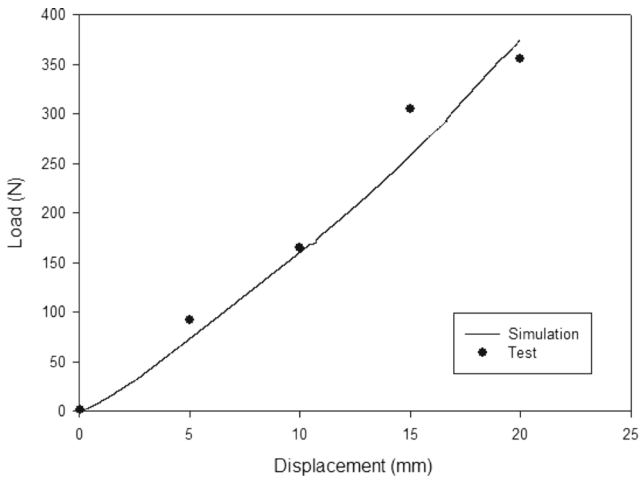

Fig. 9 Load–displacement curve obtained from indentation test

The RBF is another surrogate model that approximates multivariate functions based on scattered data by using linear combinations of a radially symmetric function based on the Euclidean distance or other such metric (Buhmann 2003). The RBF model for a dataset consisting of the values of input variables and response values at N sampling points can be expressed as

$$\hat{y}(x) = \sum_{i=1}^{N} \lambda_i \phi(\|x - x_i\|), \qquad (3)$$

where x is the vector of input variables, x_i is the vector of input variables at the ith sampling point, ϕ is an RBF of the Euclidean norm $\|x-x_i\| = \sqrt{(x-x_i)^T (x-x_i)}$ representing the radial distance r from the design point x to the sampling point or center x_i, and λ_i, $i = 1, N$ are the unknown interpolation coefficients. Among the RBF formulations, the multiquadratic formulation $\phi(r) = \sqrt{r^2 + c^2}$ is used in this study. The parameter c is a constant, and the choice of $c = 1$ has been found to be suitable for most function approximations (Wang et al. 2006). The unknown interpolation coefficients (λ_i, $i = 1, N$,) can be found by minimizing the residual or the sum of the squares of the deviations. This is expressed as

$$R = \sum_{j=1}^{N} \left[y(x_j) - \sum_{i=1}^{N} \lambda_i \phi(\|x - x_i\|) \right] \qquad (4)$$

The minimization equation can be written in matrix form as

$$[A]\{\lambda\} = \{y\}, \tag{5}$$

where $[A] = \phi(\|x_j - x_i\|)$, $j = 1, N$, $i = 1, N$; $\{\lambda_1, \lambda_2, \ldots, \lambda_N\}^T$, and $\{y\}^T\{y(x_1), y(x_2), \ldots, y(x_N)\}^T$.

After the surrogate models are constructed, both are used for optimization. Finally, the optimum designs from the surrogate model predictions were validated by using LS-DYNA. Figure 10 shows a flowchart for the surrogate-based optimization approach followed in this study. The use of the most accurate surrogate model in optimization does not necessarily lead to the optimum solution (Acar et al. 2011). Therefore, the optimization problems of this study are solved by using different surrogate model types, and multiple optimum candidates are obtained that correspond to each surrogate model type. Finally, the candidate with the best performance (ie, the smallest objective function) is declared to be the optimum configuration.

5 Results

This section presents the validation of the FEA simulations with experimental tests, the determination of the more critical test configuration, the accuracy of the surrogate models, and the optimization results for the critical test setup. The optimum results obtained with different surrogate models are compared. Finally, FEA is performed on the optimum designs to check the predictions of the surrogate models.

5.1 Validation of FEA simulations with experimental tests

Inclined to side and vertical drop tests were performed along with their FE simulations, as detailed in (Livermore Software Technology 2007). The critical regions especially included the components that came into contact with the bottom foam in the vertical drop test simulation. For the inclined drop test simulation, the parts of the dishwasher assembly on the inclined side were the most affected by impact with the ground, as expected. Experiments were also performed in the present study and recorded with a high-speed camera at 500 fps. The deformations were compared with the FEA simulation at certain time steps, as shown in Fig. 11. The packaging module was more strongly affected than the other parts of the dishwasher, so it was analyzed in detail. The FEA results were verified by checking the deformations of the packaging module during impact. Figures 12 and 13 shows that the numerical results agreed well with the experimental results for both the vertical and inclined drop tests, respectively.

5.2 Determination of the more critical test setup

As noted earlier, the deformation in the sidewalls is the main reason for the return of many products. Therefore, the maximum displacement to the side for the sidewalls in both the vertical and inclined drop tests are compared, as shown in Fig. 14. A larger region of the sidewall reached the critical displacement value in the inclined drop test. Moreover, the effective strain at the bottom foam is higher in the inclined drop test. This can also affect the deflection of the sidewalls. Thus, the inclined drop test setup is used to consider the optimization problem in this study.

5.3 Accuracy of the surrogate models

The dogleg plate thickness (t), foam density (ρ), and increment in the bottom foam height (h) are used as design variables, which served as the inputs for the surrogate models. The lower and upper bounds of these input variables are set to 1.5 mm $\leq t \leq$ 2.5 mm, 10 kg/m^3 $\leq \rho \leq$ 40 kg/m^3, and $0 \leq h \leq 5$ mm. The baseline geometry has the following values for the design variables: (1) $t = 2$ mm, (2) $\rho = 22$ kg/m^3, and (3) $h = 0$.

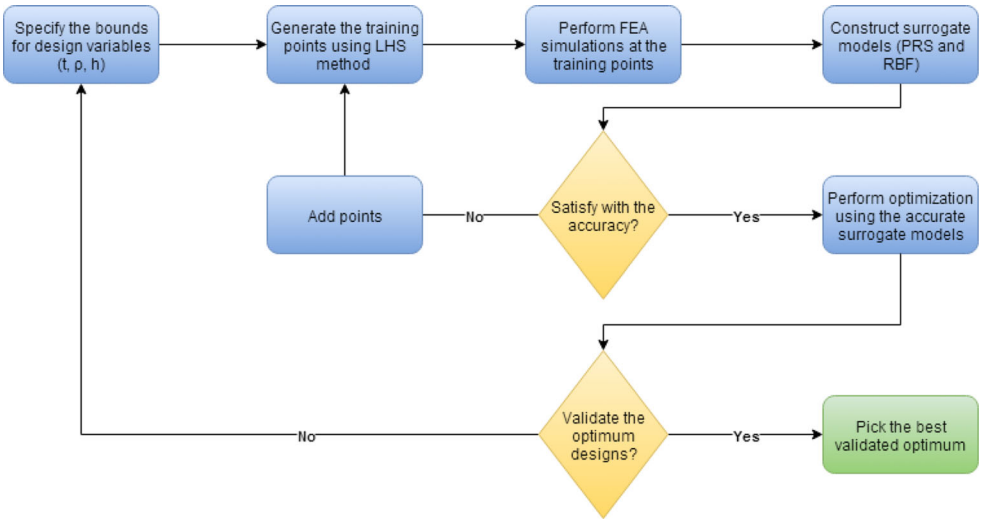

Fig. 10 Flowchart for performing surrogate-based optimization

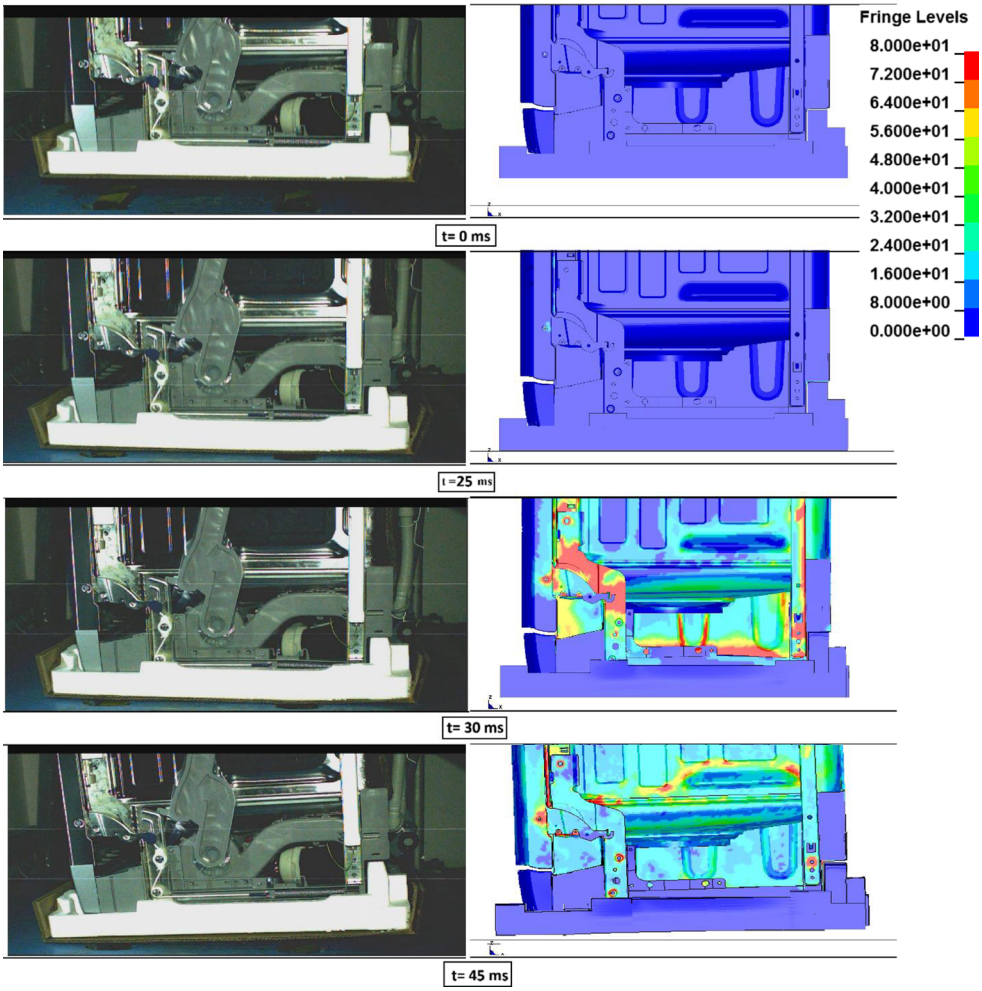

Fig. 11 Comparison of vertical drop test with FEA results (effective stress contour in MPa)

The LHS DoE is used to generate 30 training points. Then, FEA simulations are performed to compute the following constraints: (1) the maximum displacement to the side at the dogleg plate u_y, (2) the maximum displacement to the side at the sidewalls v_y, (3) the absorbed energy at the bottom foam E_A, and (4) the effective strain at the bottom foam E_S. Table 2 provides the baseline values of these constraints (columns 4–7).

Second-order PRS and RBF models are constructed to predict the responses under constraints, as discussed above. To facilitate graphical depiction, it is not possible to generate plots of surrogate models with more than two variables. Therefore, six different two-variable combinations are considered for this three-variable problem. Figures 15 and 16 plot the constructed surrogate models for displacements to the sides at the dogleg plate and

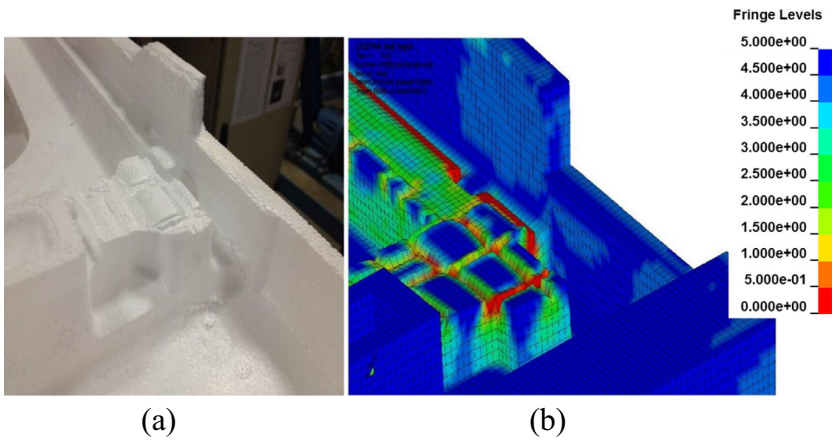

Fig. 12 Comparison of the deformed geometry of the bottom foam after vertical drop test: (**a**) Experimental result (**b**) Simulation result (effective stress contour in MPa)

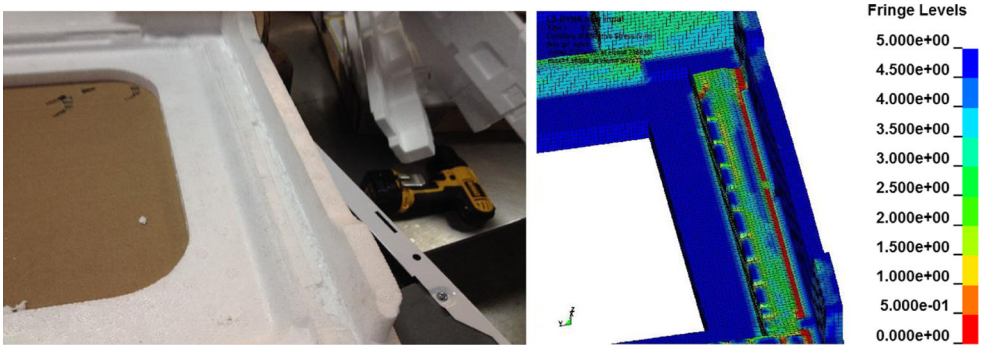

Fig. 13 Comparison of the deformed geometry of the bottom foam after inclined drop test: (**a**) Experimental result (**b**) Simulation result (effective stress contour in MPa)

sidewall, respectively. Each figure shows one design variable fixed to its midpoint value, and the other two design variables are varied within their lower and upper bounds. Appendix A provides the plots of the constructed surrogate models for the absorbed energy and effective strain at the bottom foam.

The accuracy of the PRS model at the training points is evaluated by using the root mean square error (RMSE) metric, which is used to measure the difference between values predicted by the surrogate model and the values observed in the simulations being modeled. The RMSE of a model prediction at the training points for PRS with respect to the input vector x_i is defined as

$$RMSE = \sqrt{\frac{\sum_{i=1}^{n}\left(y_i - \hat{y}\right)^2}{n}}, \tag{6}$$

where n is the number of training points and $\hat{y}_i$ is the response surface approximation at the ith training point y_i. RMSE values are normalized with respect to the ranges of responses evaluated at training points:

$$NRMSE = \frac{RMSE}{y_{\max} - y_{\min}} \tag{7}$$

Table 3 gives the normalized RMSE values for all of the responses. For the PRS model, the RMSE values for all responses are smaller than 4 %, which indicates very good accuracy. Because an RBF model passes through all of the training points, its accuracy can either be evaluated by predicting the response at randomly selected test points (requires additional response evaluations) or using cross-validation errors. The latter option is used in this study.

The accuracies of the constructed surrogate models are also evaluated by using the leave-one-out generalized mean square cross-validation error metric GMSE. If there are n training points, a surrogate model type is constructed n times; each time, one of the training points is left out. Then, the difference between the actual response y^i at the omitted training point x_i and the predicted value of the response using the surrogate model is calculated. Thus, GMSE is calculated from

$$GMSE = \frac{1}{n}\sum_{i=1}^{n}\left(y^i - \hat{y}^{(i)}\right)^2 \tag{8}$$

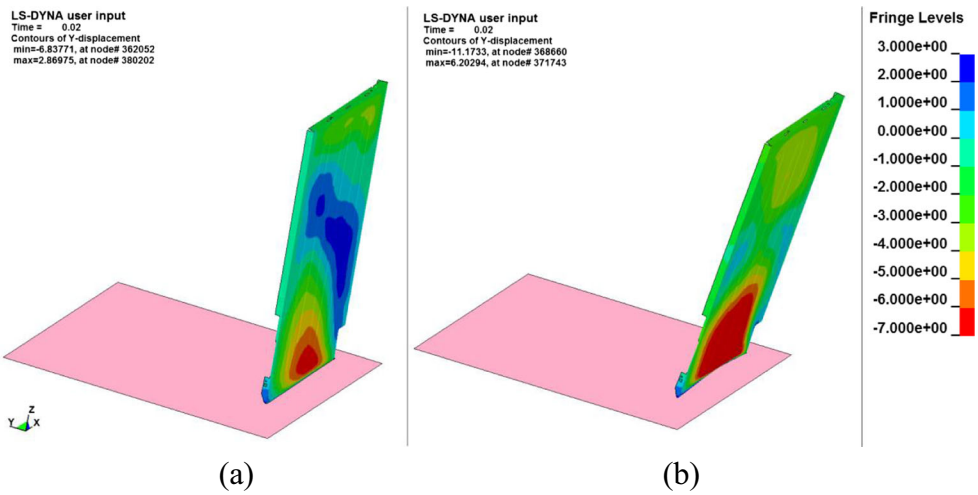

Fig. 14 Deflection of the sidewall at the point of contact ($t = 20$ ms): (**a**) Vertical drop test result (**b**) Inclined drop test result (displacement contour in mm)

Table 2 Baseline values of design variables and constraints

Design variables (x)			Constraints			
t (mm)	rho (kg/m^3)	h (mm)	u_y (mm)	v_y (mm)	E_A (J)	E_S (−)
2	22	0	2.239	11.17	27.90	2.096

GMSE values are normalized with respect to the ranges of responses evaluated at training points:

$$NGMSE = \frac{GMSE}{y_{\max} - y_{\min}} \tag{9}$$

Table 4 compares the NGMSE of the surrogate models. GMSE values are normalized with (9) and are given in Table 4. The RBF model is more accurate than PRS for the response of the first constraint (u_y), whereas the PRS model is more accurate for the responses of the other constraints. All GMSE values in Table 4 except for that of the RBF for E_S are less than 10 %, which indicates good accuracy. The GMSE of the RBF for E_S is 13.3 %, which is reasonable for a nonlinear problem.

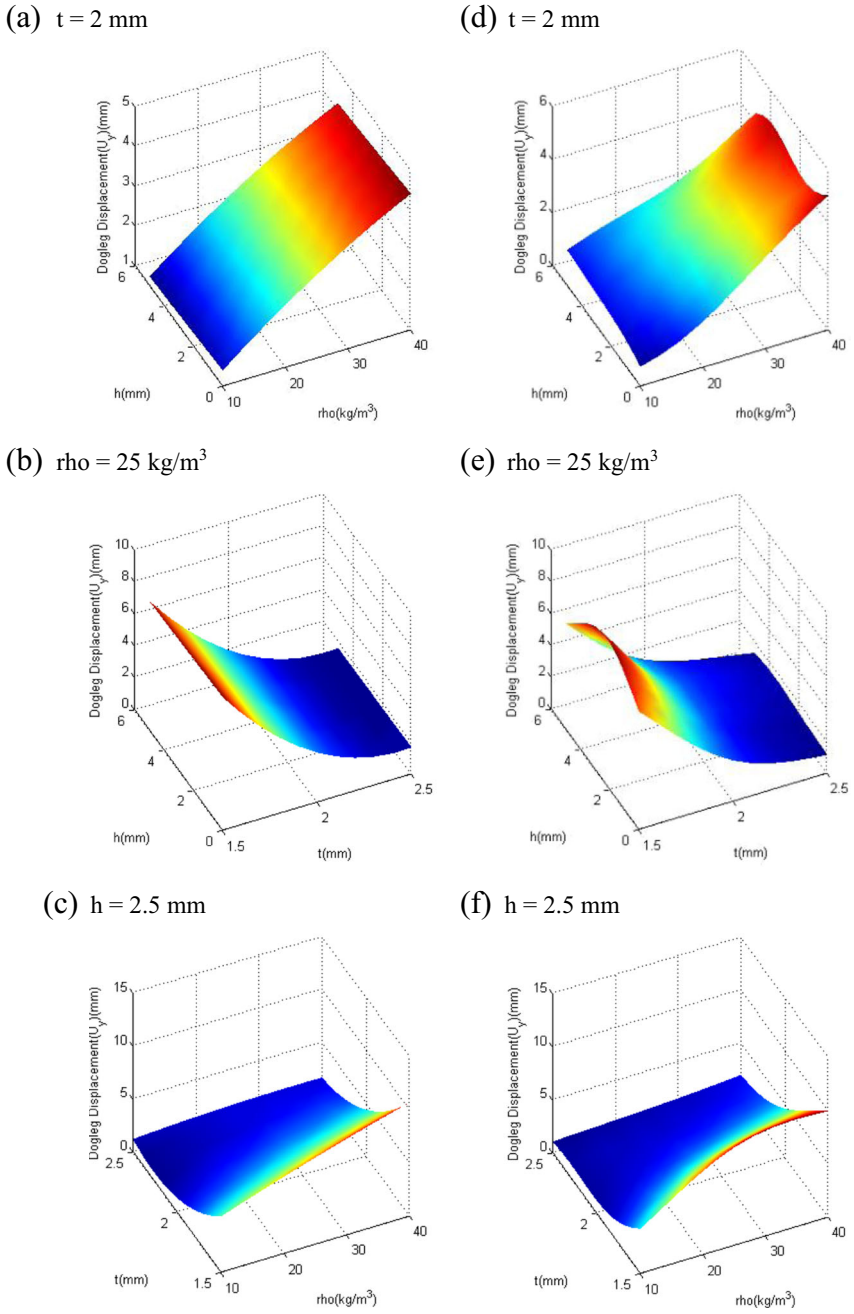

Fig. 15 Surrogate models for displacement to the side at the dogleg plate: (**a**)-(**c**) PRS and (**d**)-(**f**) RBF

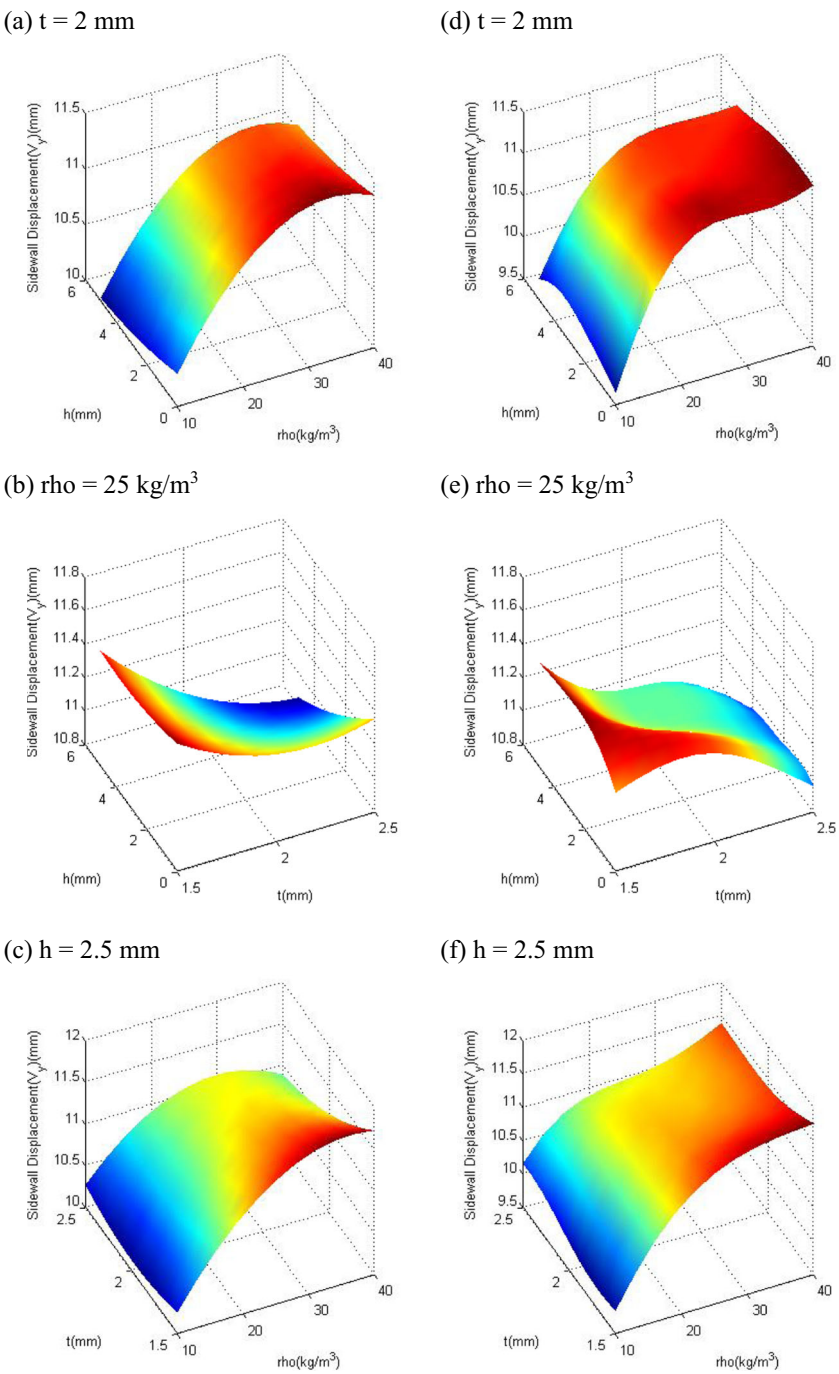

Fig. 16 Surrogate models for displacement to the side at the sidewall: (**a**)-(**c**) PRS and (**d**)-(**f**) RBF

Table 3 Accuracies of surrogate models at the training points

Surrogate model	u_y NRMSE (%)	v_y NRMSE (%)	E_A NRMSE (%)	E_S NRMSE (%)
PRS	3.40	0.71	2.09	3.96
RBF	-	-	-	-

Table 4 Accuracies of surrogate models evaluated by GMSE

Surrogate model	u_y NGMSE (%)	v_y NGMSE (%)	E_A NGMSE (%)	E_S NGMSE (%)
PRS	5.55	**5.79**	**3.20**	**7.39**
RBF	**4.45**	8.62	4.81	13.3

5.4 Optimization results

5.4.1 Single objective optimization

Each surrogate model is used separately to minimize the weight of the dogleg plate (W_d) and weight of the bottom foam (W_b). Table 5 lists the optimum configurations (see columns 3–5). The optimum design variables for both objective functions corresponding to the PRS are the same, while the RBF results are not. The RBF model provides more weight reductions for both objective functions.

FEA simulations of the optimum configurations obtained with surrogate-based optimization are performed to compute the actual values of the constraints; the results are given in Tables 6 and 7. In Table 6, positive errors indicate that the predicted responses are conservative, whereas negative errors indicate non-conservative predictions. Recall that the baseline value of u_y was 2.239 mm and v_y was 11.17 mm. Table 6 indicates positive errors for the predicted u_y, so the optimum configurations are conservative. Although the predicted v_y values were slightly non-conservative, they are all smaller than that of the baseline design. This indicates that the obtained optimum configurations are feasible in terms of v_y constraint. The RBF model provides more accurate predictions for both constraints compared to the PRS model.

In Table 7, negative errors for E_A indicate that the predictions are conservative, whereas positive errors indicate non-conservative predictions. In contrast, negative errors for E_S indicate non-conservative predictions, and positive errors indicate conservative predictions. Recall that the baseline value of E_A was 27.90 J and that of E_S was 2.096. Table 7 indicates that the E_A values predicted by both the PRS and RBF models are slightly conservative. The PRS predictions of E_S are slightly conservative, and the RBF predictions are slightly non-conservative. However, the level of non-conservatism is less than 0.1 %, so the obtained optimum configurations are reasonable.

5.4.2 Multi-objective optimization

The optimum configurations obtained from the PRS model for both objective functions yielded the same result, while those from the RBF model did not. Thus, in addition to optimizing the model for either the minimum W_d or minimum W_b with the RBF model, a composite objective function providing a compromise between W_d and W_b is optimized. This composite objective function can be defined as

$$f = w\frac{W_d}{W_{d,0}} + (1-w)\frac{W_b}{W_{b,0}}, \tag{10}$$

where f is the composite objective function to be minimized and w is a weight factor used to adjust the importance of W_d and W_b relative to each other. $W_{d,0}$ and $W_{b,0}$ are the normalization constants taken as the minimum W_d and W_b values obtained at the training points (232.7 g and 113.8 g, respectively). The case where W_d and W_b are equally important is considered, so the weight factor in (10) is set to $w = 0.5$. Table 8 lists the optimization results. The weight reduction of the bottom foam is much greater than that of the dogleg plate when W_d and W_b are equally important.

Tables 9 and 10 give the responses of the constraints corresponding to the optimum configurations. As noted for the single-objective optimization, positive errors for u_y, v_y, and E_S and a negative error for E_A indicate that the predictions are conservative. Tables 9 and 10 indicate that the predicted

Table 5 Optimization results for single objective cases

Surrogate model	Objective function	Design variables (x)			Objective function (mass) (g)			
		t (mm)	*rho* (kg/m^3)	h (mm)	Baseline	via Surrogate	via FEA	Weight reduction (%)*
PRS	min W_b	1.894	14.94	4.973	221.7	171.8	172.7	22.09
	min W_d	1.894	14.94	4.973	307.6	291.4	292.2	5.00
RBF	min W_b	2.125	14.88	3.953	221.7	166.7	166.7	**24.81**
	min W_d	1.881	16.39	4.322	307.6	289.3	289.3	**5.950**

* Weight reduction$(\%) = \frac{\text{Baseline}-\text{FEA}}{\text{Baseline}} \times 100$.

Table 6 Maximum displacement to the side at the dogleg plate, u_y and maximum displacement to the side at the sidewall, v_y for optimum configurations for single objective cases

Surrogate model	Objective function	u_y (mm)*			v_y (mm)**		
		via Surrogate	via FEA	Error *** (%)	via Surrogate	via FEA	Error (%)
PRS	min W_b	2.239	2.129	+5.20	10.54	10.70	−1.47
	min W_d	2.239	2.129	+5.20	10.54	10.70	−1.47
RBF	min W_b	1.559	1.501	+0.52	10.68	10.73	−0.47
	min W_d	2.239	2.212	+1.23	10.74	10.76	**−0.23**

* Baseline value of maximum displacement to the side at the dogleg plate, u_y is 2.239 mm

** Baseline value of maximum displacement to the side at the sidewall, v_y is 11.17 mm

*** Error (%) = (Surrogate – FEA) / FEA

Table 7 Absorbed energy at the bottom foam, *E_A* and effective strain at the bottom foam, *E_S* values for optimum configurations for single objective cases

Surrogate model	Objective function	E_A (J)*			E_S (−)**		
		via Surrogate	via FEA	Error (%)	via Surrogate	via FEA	Error (%)
PRS	min W_b	28.53	28.54	**−0.05**	2.096	2.080	+0.77
	min W_d	28.53	28.54	**−0.05**	2.096	2.080	+0.77
RBF	min W_b	28.85	29.01	−0.55	2.096	2.098	**−0.10**
	min W_d	28.44	28.40	+0.16	2.096	2.088	+0.37

* Baseline value of absorbed energy at the bottom foam, *E_A* is 27.90 J

** Baseline value of effective strain at the bottom foam, *E_S* is 2.096

v_y and E_S values are slightly non-conservative, while the predicted u_y and E_A values are conservative. The v_y and E_s values were less than those of the baseline design, which indicates that the obtained optimum configuration is feasible in terms of both constraints.

Finally, the Pareto optimal set is obtained by solving the multi-objective optimization problem for various values of the weight factor w in (10) between 0 and 1. Figure 17 depicts the Pareto optimal front (POF) obtained with the RBF model by showing the relation between W_d and W_b. The POF is linear over a small region. A small increase in the weight of the dogleg plate considerably reduces the weight of the bottom foam. Figure 16 also shows that the POF converges to a utopia point when W_d and W_b are equally important ($w = 0.5$).

6 Conclusion

This paper presents drop test simulations on the redesigned mechanical structure of a dishwasher and surrogate-based optimization of the dishwasher model and its packaging module. Vertical and inclined drop tests were considered as drop scenarios. The simulation results were compared with the experimental drop test results, and good agreement was observed.

Because the deformation in the sidewalls is the main reason for the return of many products, the sidewalls were analyzed in detail for both drop scenarios. The optimization problem focused on the inclined drop test setup because this produced the maximum displacements of the sidewalls to the side.

The thickness of the dogleg plate, density of the bottom foam, and increment in the bottom foam height were selected

Table 8 Optimization result for composite objective function

Objective function	Design variables (x)			Component	Objective function (mass) (g)			
	t (mm)	*rho* (kg/m^3)	h (mm)		Baseline	via Surrogate	via FEA	Weight reduction (%)*
min f ($w = 0.5$)	1.954	15.48	3.911	Bottom Foam	221.7	173.2	174.1	21.46
				Dogleg Plate	307.6	300.5	300.5	2.30

* Weight reduction$(\%) = \frac{\text{Baseline} - \text{FEA}}{\text{Baseline}} \times 100$

Table 9 Maximum displacement to the side at the dogleg plate, u_y and maximum displacement to the side at the sidewall, v_y for optimum configurations for composite objective function

Objective function	u_y (mm)*			v_y (mm)**		
	via Surrogate	via FEA	Error (%)	via Surrogate	via FEA	Error (%)
min $f(w=0.5)$	1.922	1.920	**+0.10**	10.70	10.76	−0.56

* Baseline value of maximum displacement to the side at the dogleg plate, u_y is 2.239 mm

** Baseline value of maximum displacement to the side at the sidewall, v_y is 11.17 mm

Table 10 Absorbed energy at the bottom foam, *E_A* and effective strain at the bottom foam, *E_S* values for optimum configurations for composite objective function

Objective function	E_A (J)*			E_S (−)**		
	via Surrogate	via FEA	Error (%)	via Surrogate	via FEA	Error (%)
min $f(w=0.5)$	28.49	28.57	−0.28	2.096	2.105	−0.43

* Baseline value of absorbed energy at the bottom foam, *E_A* is 27.90 J

** Baseline value of effective strain at the bottom foam, *E_S* is 2.096

as design variables for minimizing the weights of the dogleg plate and/or bottom foam. The PRS and RBF surrogate models were used to predict the responses under the constraints of the optimization problem.

Based on the results obtained in this study, the following conclusions were drawn:

- The weights of the dogleg plate and bottom foam could be reduced, while the optimum configuration of the dishwasher improved the crash performance.
- When a single objective was considered, the minimum weights for both components were obtained with the RBF model. The weight reduction for the dogleg plate and bottom foam were 5.95 and 24.8 %, respectively.
- When a composite objective was considered, the minimum weights for both components were obtained with the PRS model. Because the PRS model yielded the same optimum design variables for both objectives, it can also be considered as multi-objective optimization. The weight reduction for the dogleg plate and bottom foam were 5.0 and 22.9 %, respectively.

In this study, the inclined to side and vertical drop tests were considered as drop scenarios. Other drop scenarios such

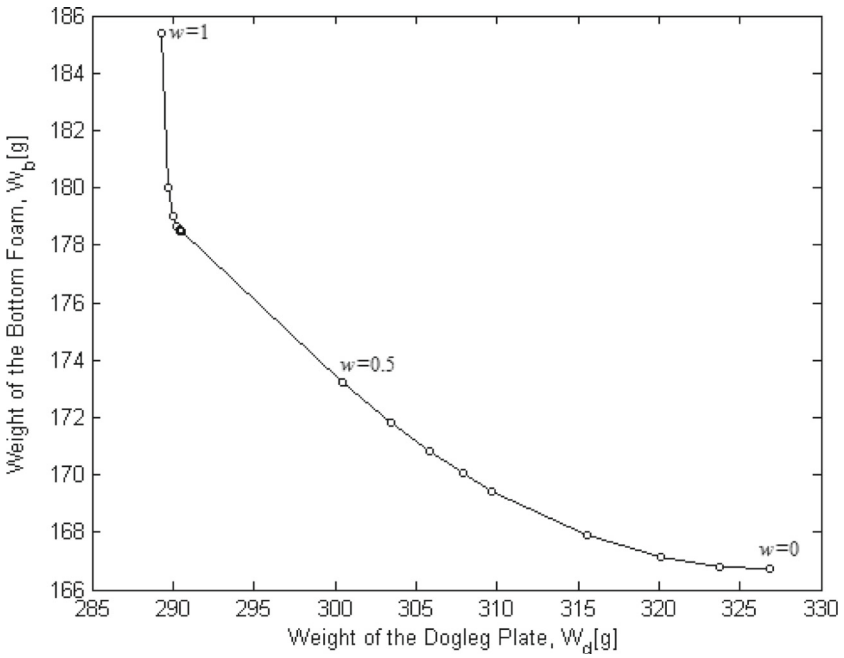

Fig. 17 The Pareto optimal front obtained using RBF model

as inclined to the front or inclined to the corner of the dishwasher can be introduced for future study. In addition, other surrogate model types such as Kriging and support vector regression can be integrated to the surrogate-based optimization approach for future work.

Acknowledgments This research was supported by TUBITAK (The Scientific and Technological Research Council of Turkey) and ARCELİK A.S. under the TEYDEB-1505 program (Project number: 5130016). The authors thank F. Ercin of ARCELIK A.S. for helping with the foam material model validation tests. The authors also thank M. Unlusoy and G.N. Naymanoglu of ARCELIK A.S. for their contributions to this study.

APPENDIX A. Constructed surrogate models

A1. The expressions of the PRS model and the coefficients of the RBF model for the responses of interest

The PRS model for the maximum displacement to the side at the dogleg plate u_y can be expressed as:

$$u_y(x) = 35.4887 - 33.5905x_1 + 0.4952x_2 - 0.1124x_3 - 0.1769x_1x_2 + 0.0390x_1x_3 - 0.0006x_2x_3 + 7.9126x_1^2 - 0.0009x_2^2 + 0.0015x_3^2 \quad \text{(A1)}$$

where the input variable vector is $x = \{t, \rho, h\}$.

The PRS model for the maximum displacement to the side at the sidewalls v_y can be expressed as:

$$v_y(x) = 10.2599 - 1.7430x_1 + 0.2113x_2 + 0.0904x_3 - 0.0304x_1x_2 - 0.0881x_1x_3 - 0.0003x_2x_3 + 0.5774x_1^2 - 0.0024x_2^2 + 0.0063x_3^2 \quad \text{(A2)}$$

The PRS model for the absorbed energy at the bottom foam E_A can be expressed as:

$$E\_A(x) = 18591 + 8372x_1 - 133x_2 - 103x_3 + 50x_1x_2 + 91x_1x_3 + 3x_2x_3 - 1581x_1^2 - x_2^2 + x_3^2 \quad \text{(A3)}$$

The PRS model for the effective strain at the bottom foam E_S can be expressed as:

$$E\_S(x) = 2.5706 - 0.1420x_1 - 0.0152x_2 - 0.0597x_3 + 0.0014x_1x_2 + 0.0228x_1x_3 + 0.0006x_2x_3 + 0.0150x_1^2 - 1.47 \times 10^{-5}x_2^2 - 0.0015x_3^2 \quad \text{(A4)}$$

The coefficients of the RBF model for the maximum displacement to the side at the dogleg plate u_y, for the maximum displacement to the side at the sidewalls v_y, for the absorbed energy at the bottom foam E_A, and for the effective strain at the bottom foam E_S are given in Tables 11-14, respectively. Surrogate models for absorbed energy and effective strain at the bottom foam are shown in Figs. 18 and 19, respectively.

Table 11 The coefficients of the RBF model for the maximum displacement to the side at the dogleg plate u_y

λ_1	35.6726	λ_{11}	−35.0873	λ_{21}	−11.5385
λ_2	6.6794	λ_{12}	−44.6100	λ_{22}	−25.0025
λ_3	10.3662	λ_{13}	111.9505	λ_{23}	16.2578
λ_4	−7.7511	λ_{14}	8.02444	λ_{24}	−15.2394
λ_5	25.2237	λ_{15}	12.1390	λ_{25}	−134.2408
λ_6	0.46144	λ_{16}	−15.5685	λ_{26}	16.8427
λ_7	34.7638	λ_{17}	−218.0256	λ_{27}	−24.5569
λ_8	−0.83543	λ_{18}	248.4971	λ_{28}	−8.8749
λ_9	−48.9991	λ_{19}	42.0071	λ_{29}	62.8018
λ_{10}	−71.7947	λ_{20}	−37.7956	λ_{30}	68.4035

Table 12 The coefficients of the RBF model for the maximum displacement to the side at the sidewalls v_y

λ_1	−3.4777	λ_{11}	−546.8331	λ_{21}	12.0784
λ_2	−119.0486	λ_{12}	−274.3191	λ_{22}	−387.9191
λ_3	43.6815	λ_{13}	118.4742	λ_{23}	132.9177
λ_4	−4.5564	λ_{14}	165.9248	λ_{24}	188.7721
λ_5	174.0896	λ_{15}	5.1152	λ_{25}	78.8297
λ_6	132.1541	λ_{16}	−52.1096	λ_{26}	−85.2178
λ_7	370.7211	λ_{17}	58.9028	λ_{27}	−476.7844
λ_8	−3.5113	λ_{18}	−329.8604	λ_{28}	−43.0776
λ_9	584.5073	λ_{19}	−5.3752	λ_{29}	26.7691
λ_{10}	−44.8441	λ_{20}	333.7835	λ_{30}	−47.8121

Table 13 The coefficients of the RBF model for the absorbed energy at the bottom foam E_A

λ_1	−30.5156	λ_{11}	121.0902	λ_{21}	19.8179
λ_2	2.6637	λ_{12}	39.3095	λ_{22}	−33.6325
λ_3	−21.0546	λ_{13}	−45.0454	λ_{23}	−11.1266
λ_4	14.4063	λ_{14}	−1.3181	λ_{24}	−48.8983
λ_5	−45.5724	λ_{15}	−9.7247	λ_{25}	108.1418
λ_6	11.1583	λ_{16}	6.6972	λ_{26}	−16.8585
λ_7	21.9125	λ_{17}	179.6243	λ_{27}	−63.2656
λ_8	5.33.52	λ_{18}	−268.7167	λ_{28}	14.1486
λ_9	145.5161	λ_{19}	−37.9661	λ_{29}	−63.1190
λ_{10}	54.9400	λ_{20}	−36.1576	λ_{30}	−9.4644

Table 14 The coefficients of the RBF model for the effective strain at the bottom foam E_S

λ_1	19.1981	λ_{11}	753.2701	λ_{21}	31.6008
λ_2	45.4378	λ_{12}	−16.8814	λ_{22}	−77.9624
λ_3	146.1826	λ_{13}	−14.3900	λ_{23}	−59.4440
λ_4	27.4731	λ_{14}	−285.3699	λ_{24}	−161.9058
λ_5	−299.7345	λ_{15}	38.8698	λ_{25}	−71.1252
λ_6	−90.6270	λ_{16}	−14.1739	λ_{26}	147.8355
λ_7	317.1662	λ_{17}	14.1825	λ_{27}	620.2359
λ_8	33.2048	λ_{18}	259.3635	λ_{28}	−41.5369
λ_9	−971.3303	λ_{19}	−39.6217	λ_{29}	−91.2928
λ_{10}	69.1438	λ_{20}	−309.9925	λ_{30}	25.2719

A.2 Absorbed energy at the bottom foam

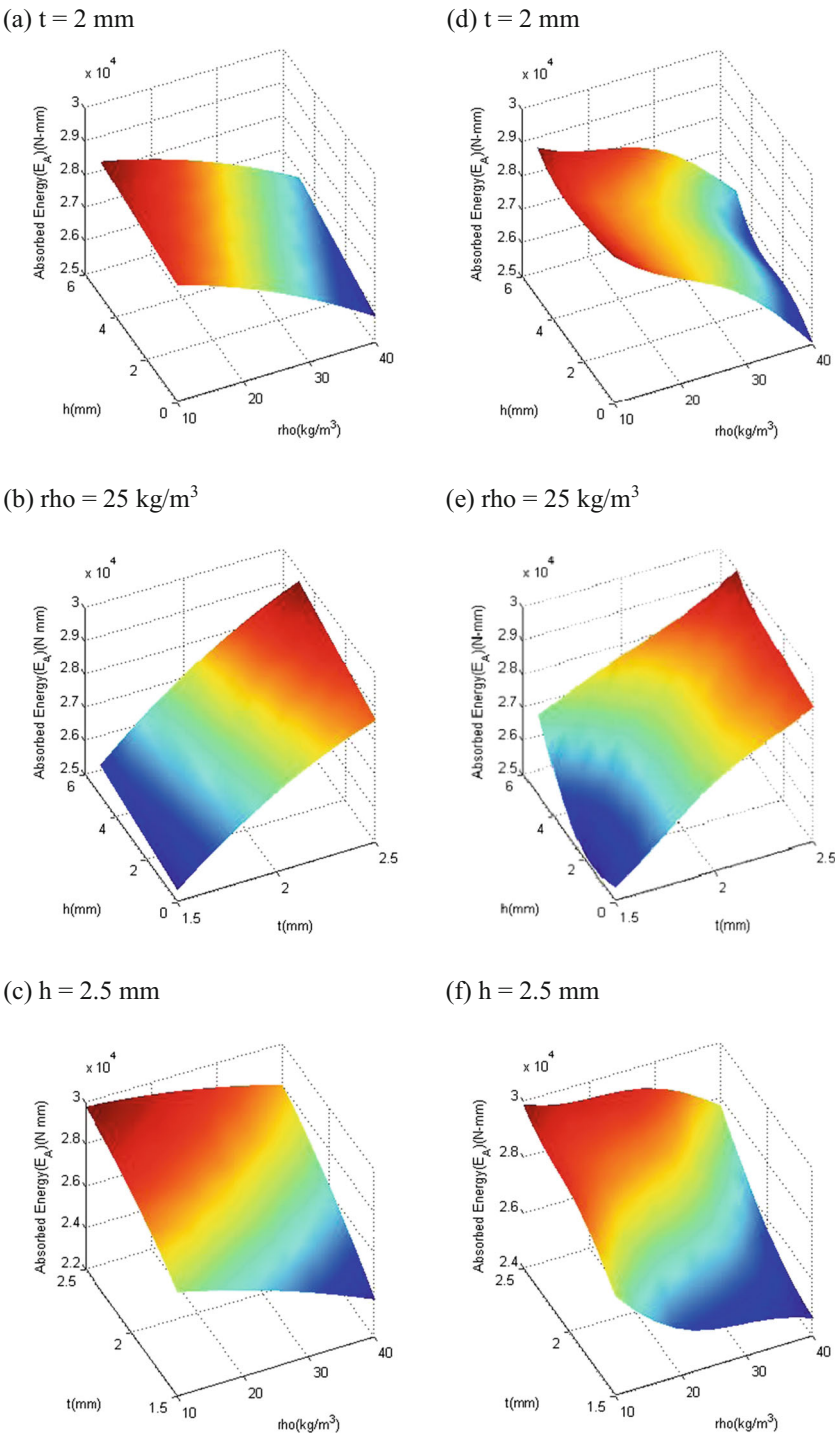

Fig. 18 Surrogate models for absorbed energy at the bottom foam: (a)-(c) PRS and (d)-(f) RBF

A.3 Effective strain at the bottom foam

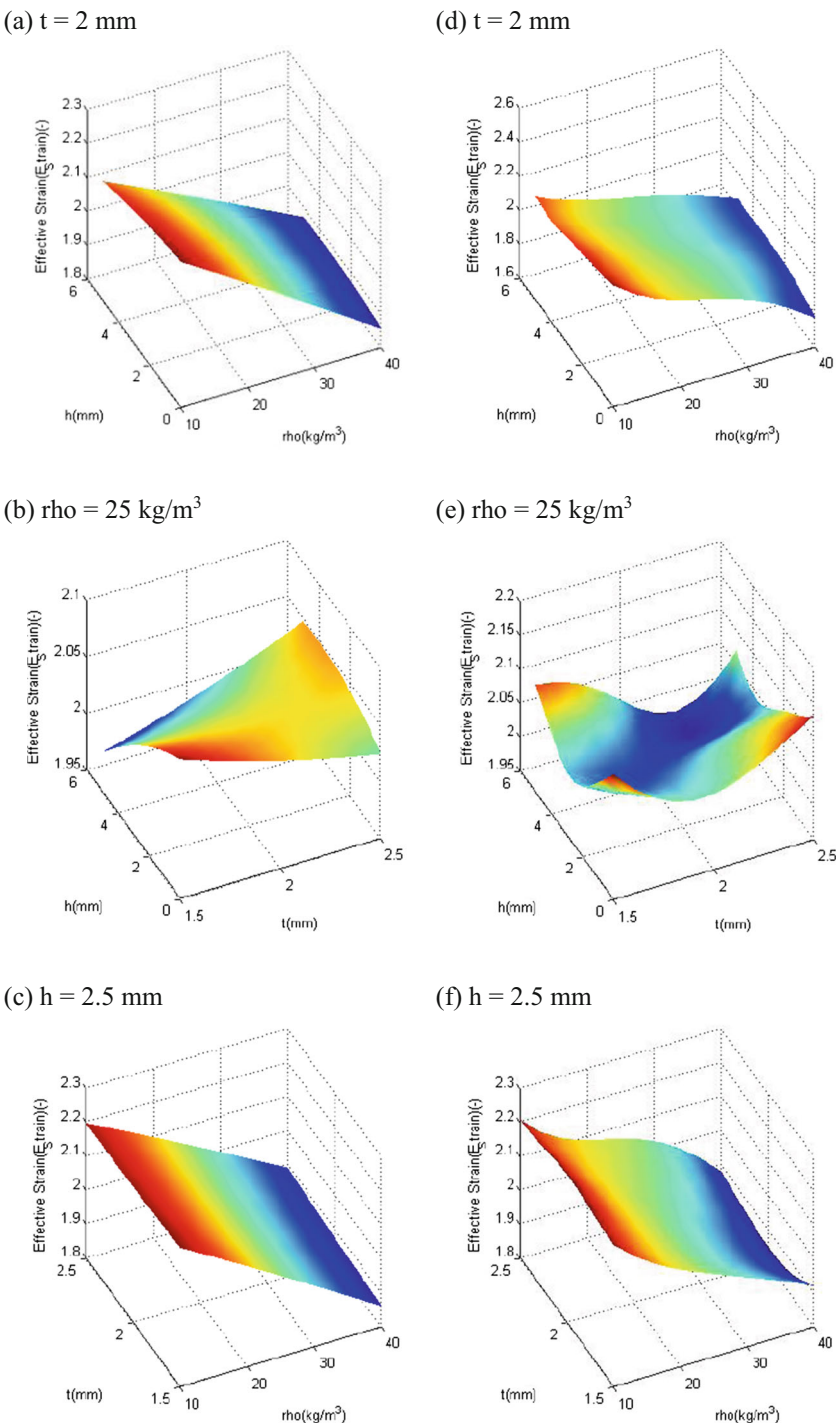

Fig. 19 Surrogate models for effective strain at the bottom foam: (a)-(c) PRS and (d)-(f) RBF

References

(2009) MATLAB user's guide and reference guide. The MathWorks Inc

Acar E, Guler MA, Gereker B, Cerit ME, Bayram B (2011) Multi-objective crashworthiness optimization of tapered thin-walled tubes with axisymmetric indentations. Thin-Walled Struct 49

Babu S, Biswas J (2008) Drop analysis of waste transfer flask, 10th Int. LS-DYNA Users Conf 57–64

Bielenberg RW, Reid JD (2004) Modeling crushable foam for the SAFER racetrack barrier, 8th Int. LS-DYNA Users Conf 1–10

Blanco DH, Ortalda A, Clementi F (2015) Impact simulations on home appliances to optimize packaging protection : a case study on a refrigerator, 10th Eur. LS-DYNA Conf

Buhmann MD (2003) Radial basis function: theory and implementations. Cambridge Univ. Press, New York, NY

Dan Neumayer (2006) Drop test simulation of a cooker including foam packaging and pre-stressed plastic foil wrapping, 9th Int. LS-DYNA Users Conf 33–40

Forrester AIJ, Sóbester A, Keane AJ (2008) Engineering design via surrogate modelling: a practical guide. John Wiley Sons, Chichester

Gunn SR (1997) Support vector machines for classification and regression, Tech. Report, Image Speech Intell. Syst. Res. Group, Univ. Southampton, UK

Huang ZL, Jiang C, Zhou YS, Luo Z, Zhang Z (2015) An incremental shifting vector approach for reliability-based design optimization. Struct Multidiscip Optim 53(3):1–21

Huang ZL, Jiang C, Zhou YS, Zheng J, Long XY (2016) Reliability-based design optimization for problems with interval distribution parameters. Struct Multidisc Optim. doi:10.1007/s00158-016-1505-3

Hwan CL, Lin MJ, Lo CC, Chen WL (2011) Drop tests and impact simulation for cell phones. J Chin Inst Eng 34:337–346

HYPERMESH, Altair Corp. S-T Mühendislik (2009) Nalbantoğlu Mah. Taşkapı Cad. Kent İş. No:18A Osmangazi, Bursa, TURKEY www.s-t.com.tr

Jackson KE, Fasanella EL (2001) Crash simulation of a vertical drop test of a B737 fuselage section with overhead bins and luggage. Int Aircr Fire Cabin Saf Res Conf

Jackson KE, Fasanella EL (2008) Development and validation of a finite element simulation of a vertical drop test of an ATR 42 Regional Transport Airplane

JEDEC Standard JESD22-B11 (2003) Board level drop test method of components for handheld electronic products, Jt. Electron Device Eng Counc

Jin R, Chen W, Simpson TW (2001) Comparative studies of metamodeling techniques under multiple modeling criteria. Struct Multi-Disciplinary Optim 23:1–13

Kim H-J, Yim J-S, Lee B-H, Oh J-Y, Tahk Y-W (2014) Drop impact analysis of plate-type fuel assembly in research reactor. Nucl Eng Technol 46:529–540

Liu W, Li H (2011) Impact analysis of a cellular phone, 4 Th ANSA μETA Int. Conf

Livermore Software Technology Corporation (2007) LS-DYNA keyword user's manual vol. I

Low KH, Wang Y, Hoon KH, Vahdati N (2004) Initial global–local analysis for drop-impact effect study of TV products. Adv Eng Softw 35:179–190

Mattila TT, Vajavaara L, Hokka J, Hussa E, Mäkelä M, Halkola V (2014) Evaluation of the drop response of handheld electronic products. Microelectron Reliab 54

MIL-STD-810F (2000) Military standard: test method standard for environmental engineering consideration and laboratory tests, US Dep. Def

MIL-STD-883F (2004) Military standard: test methods and procedures for microelectronics., Washington, DC US Off. Nav. Publ

Mulkoglu O, Guler MA, Demirbag H (2015) Drop test simulation and verification of a dishwasher mechanical structure, 10th Eur. LS-DYNA Conf

Myers RH, Montgomery DC (2002) Response Surface Methodology: process and product optimization using designed experiments. Wiley, New York, NY

Park J-S (1994) Optimal latin-hypercube designs for computer experiments. J Stat Plan Infer 111

Petkevich P, Abramov V, Yuremenko V, Piminov V, Makarov V, Afanasiev a (2014) Simulation of the nuclear fuel assembly drop test with LS-Dyna. Nucl Eng Des 269

Queipo NV, Haftka RT, Shyy W, Goel T, Vaidyanathan R, Kevin Tucker P (2005) Surrogate-based analysis and optimization. Prog Aerosp Sci 41

Sacks J, Welch WJ, Mitchell JSB, Henry PW (1989) Design and experiments of computer experiments. Stat Sci 4:409–423

Smith M (1993) Neural networks for statistical modeling. Von Nostrand Reinhold, New York

Tee TY, Ng HS, Lim CT, Pek E, Zhong Z (2004) Impact life prediction modeling of TFBGA packages under board level drop test. Microelectron Reliab 44:1131–1142

Tee TY, Luan J, Ng HS (2005) Development and application of innovational drop impact modeling techniques. Proc Electron Compon Technol 2005. ECTC'05. 504–512

Venkataraman S, Haftka RT (2004) Structural optimization complexity: what has Moore's law done for us? Struct Multidiscip Optim 28:375–387

Wang HL, Chen SC, Huang LT, Wang YC (2004) Simulation and verification of the drop test of 3C Products, 8th Int. LS-DYNA Users Conf 7–18

Wang YY, Lu C, Li J, Tan XM, Tse YC (2005) Simulation of drop/impact reliability for electronic devices. Finite Elem Anal Des 41:667–680

Wang L, Beeson D, Wiggs G, Rayasam M (2006) A comparison of metamodeling methods using practical industry requirements, Proc. 47th AIAA/ASME/ASCE/AHS/ASC Struct. Struct Dyn Mater Conf Newport, RI

Wong EH, Lim KM, Lee N, Seah S, Hoe C, Wang J (2002) Drop impact test - mechanics & physics of failure, 4th electron. Packag Technol Conf 2002:327–333

Wu J, Song G, Yeh C, Wyatt K (1998) Drop/impact simulation and test validation of telecommunication products. Intersoc Conf Therm Phenom 330–336

Yeh M-K, Huang T-H (2014) Drop test and finite element analysis of test board. Proc Eng 79:238–243

Yildiz AR, Solanki KN (2012) Multi-objective optimization of vehicle crashworthiness using a new particle swarm based approach. Int J Adv Manuf Technol 59:367–376